



ELSEVIER

Optical Materials 20 (2002) 113–118



www.elsevier.com/locate/optmat

Characterization of $\text{ZrO}_2\text{:Mn, Cl}$ luminescent coatings synthesized by the Pyrosol technique

M. García-Hipólito ^{a,b}, O. Alvarez-Fregoso ^{a,*}, E. Martínez ^a, C. Falcony ^c,
M.A. Aguilar-Frutis ^d

^a Instituto de Investigaciones en Materiales, UNAM, A.P. 70-360 Coyoacán, 04510 Mexico D.F.

^b Programa de Postgrado en Tecnología Avanzada, CICATA-IPN, Mexico

^c Departamento de Física, CINVESTAV-IPN, Apdo. Postal 14-740, 07000 Mexico D.F.

^d CICATA-IPN, Legaria, Miguel Hidalgo, 11500 Mexico D.F.

Received 3 May 2002; accepted 20 May 2002

Abstract

Manganese doped zirconia luminescent films have been deposited at temperatures ranging from 250 to 500 °C using the Pyrosol technique. The material obtained is in an amorphous state up 400 °C. For higher temperatures a polycrystalline material is obtained with a cubic and/or tetragonal crystalline zirconia phase. The photoluminescence and cathodoluminescence spectra show the bands associated with the electronic transitions ${}^4\text{T}_1({}^4\text{G}) \rightarrow {}^6\text{A}_1({}^6\text{S})$ of the Mn^{2+} ions. A decrease of the luminescence, as a function of the doping concentration, substrate temperature and electron accelerating voltage is observed. The presence of chlorine seems necessary for the red luminescence. The surface morphology of the films is also presented.

© 2002 Elsevier Science B.V. All rights reserved.

PACS: 42.70.Qs; 81.15.Rs; 78.55.-m; 78.60.Hk

Keywords: $\text{ZrO}_2\text{:Mn}$; Cl; Spray pyrolysis; Photoluminescence; Cathodoluminescence

1. Introduction

The Pyrosol (ultrasonic spray pyrolysis) method is a well-established process for depositing films [1,2]. Pyrosol technique has advantages, such as, low cost, a high deposition rate and ease of operation. This process has been used to deposit suc-

cessfully a variety of films (oxides, sulfides, etc.), especially luminescent films [3,4]. Presently, research on zirconia (ZrO_2) has attracted considerable attention in the field of ceramics technology, opto-electronic applications and protective coatings due to several of its remarkable characteristics, which make zirconia suitable for an abundant variety of applications [5,6]. Regarding to luminescent properties of zirconia, there are some studies on Tb and Eu doped luminescent zirconia single crystals and powders [7–9]. Research on luminescent zirconia films is very scarce [10,11]. Mn ions ($3d^5$ configuration) participate actively in

* Corresponding author. Tel.: +52-55-5622-4649; fax: +52-55-5616-1371.

E-mail address: oaf@servidor.unam.mx (O. Alvarez-Fregoso).

order to create very efficient luminescence centers in some hosts; moreover, they are important activators of luminescence in many commercial phosphors. The emissions of this ion can be situated in the blue, the green, the yellow-orange or the red regions depending on the host lattice and co-activator ions [12,13]. However, there are no previous reports on the incorporation of Mn in zirconia films with or without chlorine co-activator. The luminescent materials can be applied in electroluminescent flat panel displays, color plasma displays panels, fluorescent lamps, cathode ray tubes, etc. The present study is devoted to the structural, cathodoluminescent (CL) and photoluminescent (PL) characterization of $\text{ZrO}_2\text{:Mn, Cl}$ layers synthesized by the Pyrosol technique. To our best knowledge, studies on luminescent coatings of Mn doped zirconia are non-existent in the literature.

2. Experimental

The details of the Pyrosol technique have been presented elsewhere [2]. The starting materials to prepare $\text{ZrO}_2\text{:Mn, Cl}$ films were $\text{ZrOCl}_2 \cdot 8\text{H}_2\text{O}$ (Merck) and $\text{MnCl}_2 \cdot 4\text{H}_2\text{O}$ (Aldrich Chemical Co.). The molarity of the spraying solution was 0.05 M and the solvent was deionized water. MnCl_2 concentration in the spraying solution (C_{Mn}) was in the range from 1 to 20 at.% in relation to the Zr content. The carrier gas flow (air) was 12 l/min. Substrate temperature (T_s) during deposition was in the range from 250 to 500 °C; the substrates used were Corning 7059 glass slides. The deposition time was adjusted (4–6 min) in order to obtain similar thickness of all samples studied. This thickness was approximately 5 μm as measured by a Sloan Dektak IIA profilometer. The crystalline structure of the deposited films was analyzed by X-ray diffraction (XRD), using a Siemens D-5000 diffractometer ($\lambda = 1.5406 \text{ \AA}$, CuK_α). The chemical composition of the films was measured using energy dispersive spectroscopy (EDS) with a Leica-Cambridge electron microscope Mo. Stereoscan 440 (images by scanning electron microscopy, SEM, were also obtained using this apparatus). CL measurements were performed in a vacuum chamber with a cold

cathode electron gun (Luminoscope, model ELM-2 MCA, RELION Co.). The emitted light from the sample was coupled into an optical fiber bundle leading to a Perkin–Elmer LS50B fluorescence spectrophotometer. The excitation and PL spectra were obtained by means of the above-mentioned spectrophotometer. All luminescence measurements were carried out at room temperature.

3. Results and discussion

XRD measurements carried out on $\text{ZrO}_2\text{:Mn, Cl}$ ($C_{\text{Mn}} = 10 \text{ at.}\%$) films are shown in the Fig. 1. Here, diffraction patterns for samples deposited at T_s from 250 to 500 °C are presented. The zirconia coatings remain in the non-crystalline state when deposited at T_s lower than 400 °C. For higher T_s , these films revealed peaks that could be attributed to either the cubic and/or tetragonal structures since both exhibit diffraction patterns at nearly overlapping angles. Apparently, the presence of Mn and Cl ions in the zirconia contributes to stabilize the above-mentioned phases at these relatively low substrate temperatures. The XRD spectra revealed a preferred (111) orientation of zirconia normal to the film surface. Sharper diffraction peaks at high T_s could indicate an increase in the crystallite size.

The surface morphology of $\text{ZrO}_2\text{:Mn, Cl}$ ($C_{\text{Mn}} = 10 \text{ at.}\%$) coatings are presented in Fig. 2. It is pos-

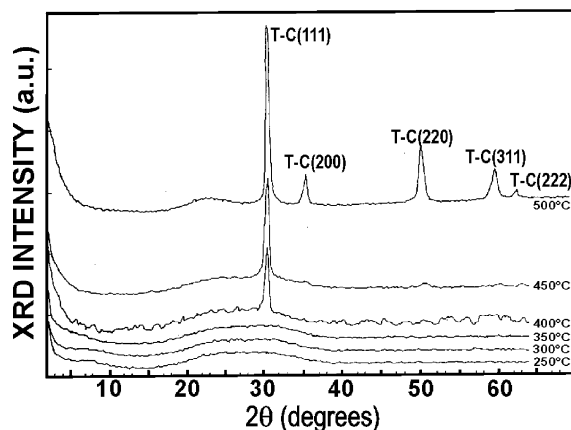


Fig. 1. XRD patterns for $\text{ZrO}_2\text{:Mn, Cl}$ films at six different T_s : 250, 300, 350, 400, 450 and 500 °C. (T = tetragonal, C = cubic).

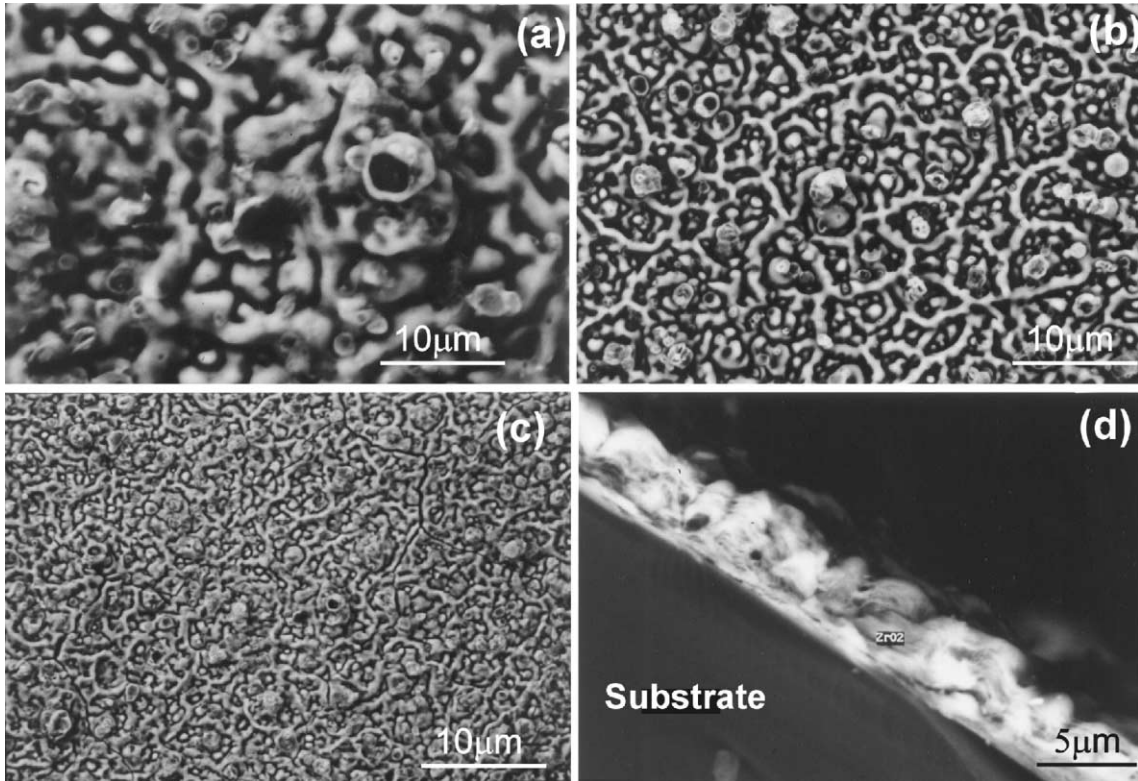


Fig. 2. SEM micrographs of $\text{ZrO}_2\text{:Mn, Cl}$ films as a function of the T_s : (a) 250 °C, (b) 400 °C, (c) 500 °C and (d) SEM image of cross-section for the film deposited at 250 °C.

sible to observe rough but continuous and crack free films with good adherence. SEM micrographs of the samples deposited at 250 °C (a), 400 °C (b) and 500 °C (c) in Fig. 2(a)–(c) indicate that the morphology of the films depended on T_s . With increasing T_s , the texture of the films changed from a porous network to a relative less rough surface and denser material than that obtained at lower T_s . A cross-sectional SEM image of the film deposited at 250 °C is presented in Fig. 2(d). In this case, the uniformity in thickness of the film can be appreciated. In addition, a nodular rather than columnar growth of the layer is observed.

EDS measurements on the chemical composition of the $\text{ZrO}_2\text{:Mn, Cl}$ samples are shown in Tables 1 and 2. The relative content of oxygen, zirconium, manganese and chlorine as a function of the C_{Mn} ($T_s = 250$ °C) are presented in Table 1. A reduction of the relative content of oxygen and

Table 1

Atomic percent content of the oxygen, zirconium, manganese and chlorine in $\text{ZrO}_2\text{:Mn, Cl}$ films as measured by EDS for different C_{Mn} , $T_s = 250$ °C

C_{Mn} (at.%)	Oxygen	Zirconium	Manganese	Chlorine
0	63.20	27.65	0.00	9.15
1	62.66	26.69	0.27	10.38
3	62.48	24.21	0.79	12.52
5	61.77	23.48	1.14	13.61
10	60.46	22.87	1.53	15.14
20	59.94	20.98	2.85	16.23

zirconium is observed, while the relative quantities of manganese and chlorine rise as the C_{Mn} increase. Table 2 shows similar data as that showed in Table 1, but as a function of the T_s , keeping constant the C_{Mn} at 10 at.%. An increase in the relative content of oxygen, zirconium and manganese is observed as T_s rises, while a remarkable

Table 2

Atomic percent content of the oxygen, zirconium, manganese and chlorine in $\text{ZrO}_2\text{:Mn, Cl}$ films as determined by EDS for different T_s , $C_{\text{Mn}} = 10$ at.%

T_s (°C)	Oxygen	Zirconium	Manganese	Chlorine
250	60.46	22.87	1.53	15.14
300	61.06	23.12	2.07	13.75
350	63.74	23.98	2.22	10.06
400	65.72	24.55	2.39	7.34
450	67.38	25.97	2.63	4.02
500	68.93	26.88	2.87	1.32

decrease of chlorine content occurs on the other hand. EDS measurements were performed on films deposited on (100)-silicon single crystals substrates in order to be able to evaluate the oxygen content in the films.

Fig. 3 shows the excitation spectrum of $\text{ZrO}_2\text{:Mn, Cl}$ coating ($T_s = 250$ °C, $C_{\text{Mn}} = 10$ at.% and $\lambda_{\text{em}} = 650$ nm), this spectrum presents three main peaks centered at 260 (highest), 335 and 378 nm, which correspond to the ${}^4\text{A}_2\text{g}({}^4\text{F})$, ${}^4\text{E}_\text{g}({}^4\text{D})$ and ${}^4\text{E}_\text{g}, {}^4\text{A}_1\text{g}({}^4\text{G})$ Mn^{2+} energy states in an octahedral crystal field, respectively [14]. These electronic levels are of even parity, since they belong to the $3d^5$ electronic configuration.

Emission spectra ($\lambda_{\text{exc}} = 260$ nm) as a function of the T_s for these films are shown in Fig. 4. A wide band centered at 650 nm corresponding to the

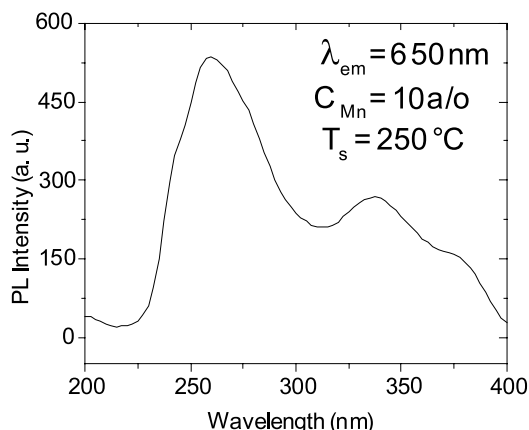


Fig. 3. Excitation spectrum of $\text{ZrO}_2\text{:Mn, Cl}$ films deposited at $T_s = 250$ °C, $C_{\text{Mn}} = 10$ at.% and $\lambda_{\text{em}} = 650$ nm.

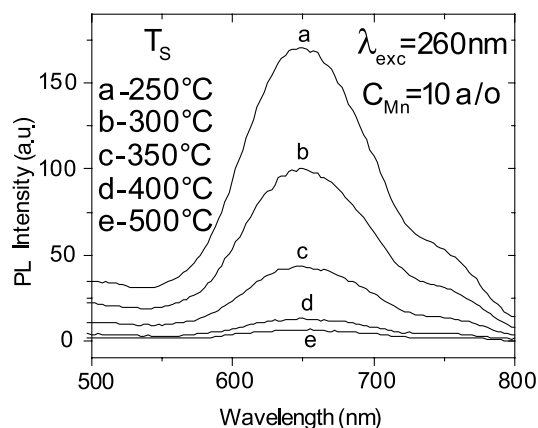


Fig. 4. PL spectra for $\text{ZrO}_2\text{:Mn, Cl}$ films as a function of the T_s . The $C_{\text{Mn}} = 10$ at.%, $\lambda_{\text{exc}} = 260$ nm.

${}^4\text{T}_1({}^4\text{G}) \rightarrow {}^6\text{A}_1({}^6\text{S})$ electronic transition of Mn^{2+} ions is observed. The PL emission intensity is reduced as the T_s are increased. This quenching effect of the PL with rise of T_s could be associated with the decrease of the Cl remaining in the film as T_s are increased (see Table 2). This correlation indicates dependence between the PL and the amount of Cl present in the films. It is possible that Cl acts as a co-activator to the Mn in order to get this red emission. Another possibility is that the manganese chloride molecule or some other compound involving Mn and Cl ions could be responsible for the red PL observed. It is known that an influence of the Cl on the Mn luminescent properties exists. In general, it has been reported that increases in either the Cl or the Mn concentration cause the peak position of the Mn^{2+} emission band to shift to longer wavelength [15]. Other mechanisms to explain this quenching behavior with deposition temperature such as Mn oxidation are possible and can not be ruled out neither confirmed with the available data. More work is required in our case to elucidate this point.

Fig. 5 shows the integrated PL intensity for the spectra of $\text{ZrO}_2\text{:Mn, Cl}$ layers, for different values of the C_{Mn} , in this case the $\lambda_{\text{exc}} = 260$ nm and $T_s = 250$ °C. The emission intensity presents a maximum for $C_{\text{Mn}} = 10$ at.% (1.53 at.% of Mn as measured by EDS) higher or lower C_{Mn} result in less intense PL emissions. The concentration quenching of the PL is due to the excess of impurities, which, under this

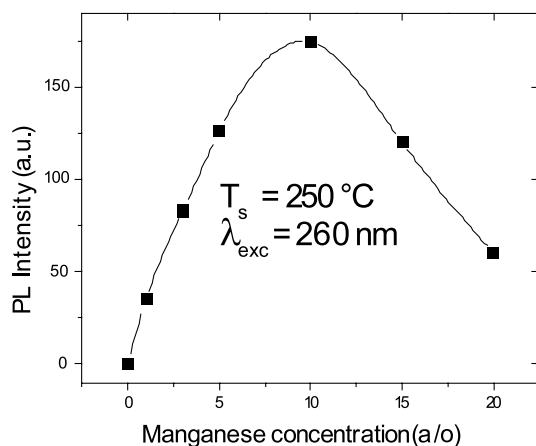


Fig. 5. Integrated PL intensity for the spectra of $\text{ZrO}_2\text{:Mn, Cl}$ films as a function of C_{Mn} . $T_s = 250^\circ\text{C}$, $\lambda_{\text{exc}} = 260\text{ nm}$. The solid line is only to guide the eye.

condition, interact with each other, generating clusters such as pairs, or triples of Mn ions what favors the dissipation of the energy by non-radiative processes [3].

Fig. 6 shows CL spectra for $\text{ZrO}_2\text{:Mn, Cl}$ films as a function of T_s ($C_{\text{Mn}} = 5\text{ at.}\%$, $V = 7\text{ kV}$). A drastic decrease of CL emission intensity as T_s rise is observed. This behavior is similar to that observed for PL emission. Probably the mechanisms responsible for the quenching of the luminescence

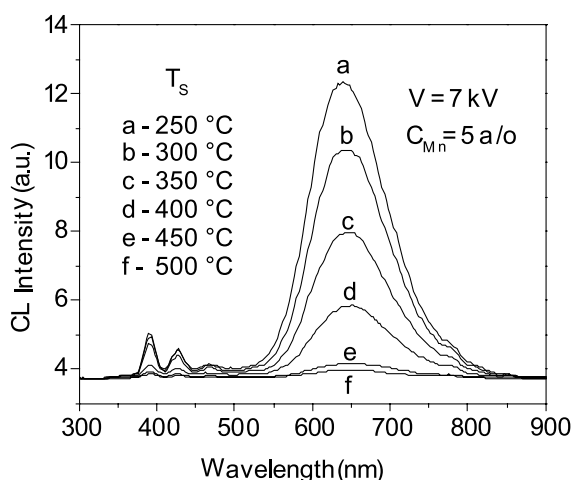


Fig. 6. CL spectra for $\text{ZrO}_2\text{:Mn, Cl}$ films as a function of the T_s , under 7 kV electron accelerating potential. $C_{\text{Mn}} = 5\text{ at.}\%$.

are associated to the presence of Cl inside the films and are similar for PL and CL.

CL spectra for $\text{ZrO}_2\text{:Mn, Cl}$ films (not shown) as a function of C_{Mn} present wide bands centered at 650 nm and other small peaks centered in the region of 400–500 nm. In general, the behavior is very similar to that obtained for the case of Fig. 6, except that optimum value for C_{Mn} was 5 at.% (1.14 at.% of Mn as measured by EDS). $T_s = 250^\circ\text{C}$ and $V = 7\text{ kV}$.

The integrated 650 nm CL intensity for the spectra of $\text{ZrO}_2\text{:Mn, Cl}$ coatings as a function of electron accelerating voltage are shown in Fig. 7 ($C_{\text{Mn}} = 5\text{ at.}\%$, $T_s = 250^\circ\text{C}$). Here, it is observed that voltages higher than 7 kV produce a substantial reduction of the 650 nm CL emission intensity. It is probable that voltages higher than 7 kV produce changes in the center responsible for red emission, which could lead to this effect. It is necessary more investigation in this regard.

Fig. 8 shows a CL spectrum for $\text{ZrO}_2\text{:Mn, Cl}$ film deposited at 500°C ($C_{\text{Mn}} = 5\text{ at.}\%$) and irradiated under 10 kV electron accelerating voltage. The strongest band centered at 590 nm corresponds to the typical yellow-orange emission arising from ${}^4T_1({}^4G) \rightarrow {}^6A_1({}^6S)$ (d–d) transition of the octahedrally coordinated Mn^{2+} ion. It is remarkable to point out that, in this case, CL emissions were not observed for accelerating potentials lower than

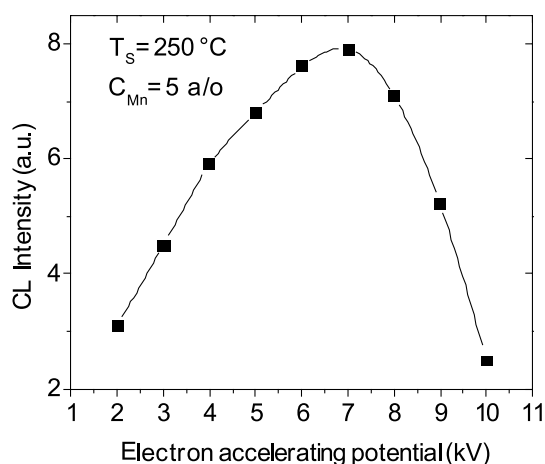


Fig. 7. Integrated CL intensity for the spectra of $\text{ZrO}_2\text{:Mn, Cl}$ films as a function of the electron acceleration voltage. $T_s = 250^\circ\text{C}$, $C_{\text{Mn}} = 5\text{ at.}\%$. The solid line is only to guide the eye.

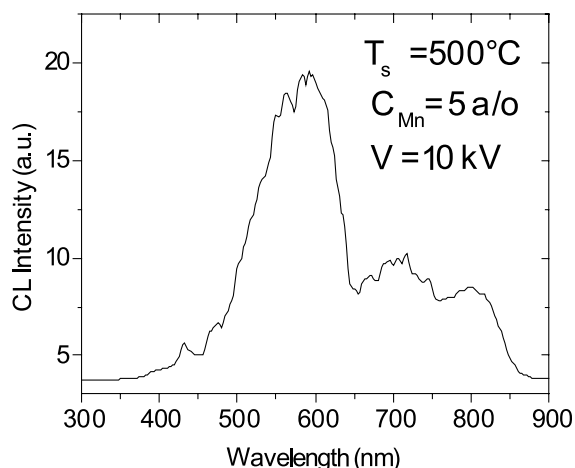


Fig. 8. CL spectrum for $\text{ZrO}_2\text{:Mn, Cl}$ film deposited at $500\text{ }^\circ\text{C}$, under 10 kV electrons accelerating potential. $C_{\text{Mn}} = 5\text{ at.}\%$.

10 kV . This sample has a relative minor amount of Cl and consequently the red emission is not present but yellow-orange emissions appear. This behavior is not observed for samples deposited at lower substrate temperatures. More studies are in process regarding this interesting point.

4. Conclusions

In conclusion, the present investigation have shown that good-quality PL and CL $\text{ZrO}_2\text{:Mn, Cl}$ coatings have been deposited by the Pyrosol technique. The crystalline properties and surface morphology of the films depend on T_s . A high deposition rate up to $1\text{ }\mu\text{m}$ per min was observed. The $\lambda_{\text{exc}} = 260\text{ nm}$ originate the strongest red emission intensity in PL. Both PL and CL red emission intensities depend on T_s and C_{Mn} . Concentration quenching of CL and PL occurs at activator concentration greater than 1.14 and 1.53 at.%, respectively. The presence of Cl is necessary to generate the red emission. A yellow-orange CL emission was obtained for samples deposited at $500\text{ }^\circ\text{C}$ and electron accelerating potentials ≥ 10

kV . From the reported results in this paper, it is clear that zirconia make efficient and interesting host for Mn^{2+} ions. Therefore, $\text{ZrO}_2\text{:Mn, Cl}$ coatings emitting in red and yellow-orange colors, have been synthesized for the first time to our knowledge.

Acknowledgements

The authors thank L. Baños and J. Guzmán for XRD and SEM-EDS measurements, respectively. In addition, we thank M. Guerrero, Sara Jimenez and J. García for technical supports.

References

- [1] J.C. Viguie, J. Spitz, *J. Electrochem. Soc.* 122 (1975) 585.
- [2] M. Langlet, J.C. Joubert, in: C.N.R. Rao (Ed.), *Chemistry of Advanced Materials*, Blackwell Science, Oxford, England, 1993, p. 55.
- [3] C. Falcony, M. García, A. Ortiz, J.C. Alonso, *J. Appl. Phys.* 72 (1992) 1525.
- [4] A. Ortiz, C. Falcony, J. Hernández- A, M. García, J.C. Alonso, *Thin Solid Films* 293 (1997) 103.
- [5] J.W. Fairbanks, R.J. Hecht, *Mater. Sci. Eng.* 88 (1987) 273.
- [6] K. Ohta, K. Yamada, K. Shimizu, T. Ozawa, *Solid State Ionics* 3–4 (1982) 443.
- [7] D. Hartmann, *Z. Phys. Chemie* 256 (1975) 97.
- [8] D. Van der Voort, G. Blasse, *Chem. Matter.* 3 (1991) 1041.
- [9] A. Gedanken, R. Reisfeld, E. Sominiski, O. Palchik, Yu. Kolytyn, G. Panczer, M. Gaft, H. Minti, *J. Phys. Chem. B* 104 (2000) 7057.
- [10] R. Reisfeld, M. Gaft, T. Saridarov, G. Panczer, M. Zelner, *Mater. Lett. B* 45 (2000) 154.
- [11] E. Pereyra-Perea, M.R. Estrada-Yañez, M. García, *J. Phys. D: Appl. Phys.* 31 (1998) L7.
- [12] G.F. Inbusch, in: M.D. Lump (Ed.), *Luminescence Spectroscopy*, Academic Press, New York, 1978 (Chapter 1).
- [13] S. Shionoya, in: D.R. Vij (Ed.), *Luminescence of Solids*, Plenum Press, New York, 1998 (Chapter 3).
- [14] L.J. Heidt, G.F. Koster, A.M. Johnson, *J. Am. Chem. Soc.* 80 (1958) 6471.
- [15] T.E. Peters, R.G. Pappalardo, R.B. Hunt Jr., in: M.D. Lump (Ed.), *Luminescence Spectroscopy*, Academic Press, New York, 1978 (Chapter 10).